High Energy Density Physics 9 (2013) 192–197

Contents lists available at SciVerse ScienceDirect

High Energy Density Physics

journal homepage: www.elsevier.com/locate/hedp

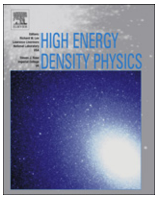

Simulation of laser-driven, ablated plasma flows in collisionless shock experiments on OMEGA and the NIF

M.J. Grosskopf[a,*], R.P. Drake[a], C.C. Kuranz[a], E.M. Rutter[a], J.S. Ross[b], N.L. Kugland[b], C. Plechaty[b], B.A. Remington[b], A. Spitkovsky[c], L. Gargate[c], G. Gregori[d], A. Bell[d], C.D. Murphy[d], J. Meinecke[d], B. Reville[d], Y. Sakawa[e], Y. Kuramitsu[e], H. Takabe[e], D.H. Froula[f], G. Fiksel[f], F. Miniati[g], M. Koenig[h], A. Ravasio[h], E. Liang[i], W. Fu[i], N. Woolsey[j], H.-S. Park[b]

[a] *University of Michigan, Ann Arbor, MI, USA*
[b] *Lawrence Livermore National Laboratory, Livermore, CA, USA*
[c] *Princeton Univertsity, Princeton, NJ, USA*
[d] *University of Oxford, Oxford, Oxfordshire, England, UK*
[e] *Osaka University, Suita, Osaka, Japan*
[f] *Laboratory for Laser Energetics, Rochester, NY, USA*
[g] *ETH Science and Technology University, Zurich, Switzerland*
[h] *Ecole Polytechnique, Palaiseau, France*
[i] *Rice University, Houston, TX, USA*
[j] *University of York, York, England, UK*

ARTICLE INFO

Article history:
Received 12 June 2012
Received in revised form
15 October 2012
Accepted 27 November 2012
Available online 4 January 2013

Keywords:
Collisionless shocks
Computational models
Laboratory astrophysics

ABSTRACT

Experiments investigating the physics of interpenetrating, collisionless, ablated plasma flows have become an important area of research in the high-energy-density field. In order to evaluate the feasibility of designing experiments that will generate a collisionless shock mediated by the Weibel instability on the National Ignition Facility (NIF) laser, computer simulations using the Center for Radiative Shock Hydrodynamics (CRASH) radiation-hydrodynamics model have been carried out. This paper reports assessment of whether the experiment can reach the required scale size while maintaining the low interflow collisionality necessary for the collisionless shock to form. Comparison of simulation results with data from Omega experiments shows the ability of the CRASH code to model these ablated systems. The combined results indicate that experiments on the NIF are capable of reaching the regimes necessary for the formation of a collisionless shock in a laboratory experiment.

1. Introduction

Collisionless shocks are ubiquitous in astrophysics and have recently become an active area of research in high-energy-density laboratory experiments. In astrophysics and space science, nearly all shock waves that one can readily detect are collisionless [1,2]. Examples include shocks in supernova remnants [3] and shocks where the solar wind encounters planetary magnetospheres [4]. In the laboratory, recent years have seen increasing activity in experimental design [5–7] and results [8–13]. Our focus here is on collisionless shocks that develop and endure in initially unmagnetized, interpenetrating plasma flows. An electrostatic shock may initially form in such interpenetrating flows, if the Mach number is small enough [14,15]. But Particle In Cell (PIC) simulations indicate that such shocks saturate and then dissipate in time [16], so such shocks do not appear to endure. On an intermediate timescale, the Weibel instability can arise, producing a structured magnetic field that randomizes that particle motion to create a Weibel-mediated shock [17]. The Weibel instability is driven by anisotropy in the particle distribution functions, definitely present in interpenetrating plasma flows, and it is specifically the response to anisotropic ion distributions that may produce shock waves. Weibel-mediated shocks have long been recognized to be potentially important [4], and in recent years have specifically been hypothesized to play an important role in gamma-ray bursts [18]. Such shocks have the potential to endure, and the work discussed here is part of the effort to develop experiments that can produce and observe Weibel-mediated shocks.

---

[*] Corresponding author.
E-mail address: mikegros@umich.edu (M.J. Grosskopf).

1574-1818/$ – see front matter Published by Elsevier B.V.
http://dx.doi.org/10.1016/j.hedp.2012.11.004

Accomplishing the goal of producing and observing Weibel-mediated shocks has several facets. We present here results from one facet of this effort – radiation-hydrodynamic simulations – but first set the context by discussing the other facets. The potential that one might be able to observe Weibel-mediated shocks in laboratory experiments was first identified by Kato and Takabe [19] based on PIC simulations. This work and subsequent PIC simulations [20–24], all in uniform plasmas, showed that the size of the system required to develop Weibel-mediated shocks was about 300 ion skin depths. The figures in these papers show the microscopic field and plasma structures that develop. The need is to have a large enough plasma to develop Weibel generated magnetic fields that then randomize the ion motion – there is no sharp threshold for shock formation. Analytic and semi-analytic design work [6,25,26], discussed further below, showed that one was likely to be able to produce Weibel-mediated shocks in the laboratory, but that meeting all the necessary constraints would probably require a laser facility on the scale of the National Ignition Facility (NIF). Meanwhile experiments, also discussed further below, began to develop diagnostic methods and experimental technique that could be used on larger systems. This included the application of proton radiography in this context [27]; proton radiography is the most likely diagnostic to be used in such experiments on NIF. However, PIC simulations cannot model plasma of interest on a realistic space and timescale, the analytic theory cannot determine the plasma conditions that will exist in a given experiment, and the experiments being done to date produce conditions that are not expected to create Weibel-mediated shocks. One also needs an assessment of whether the required plasma conditions can be produced on NIF, and this is the contribution that radiation-hydrodynamic simulations can make. Such simulations cannot directly model the Weibel instability, nor can they model the interpenetration of plasmas (since they model *hydrodynamic* behavior). What they can do is to calculate the laser energy deposition, the resulting plasma expansion, and the properties of the expanding plasma. One can then evaluate these results in the context of the constraints for collisionless shock formation determined from the PIC simulations and semi-analytic design work. This paper presents the results of such simulations, along with results of simulations indicating the ability of CRASH to accurately model existing experiments. We reach the conclusion that on NIF one would expect to be able to produce Weibel-mediated shocks.

2. Experimental campaign investigating weakly-collisional interpenetrating ablated plasma flows

The Astrophysical Collisionless Shock Experiments with Lasers (ACSEL) collaboration has carried out a series of experimental campaigns at large laser facilities aimed at understanding magnetogenesis in high-energy plasma conditions relevant to astrophysical systems. Kuramitsu et al. carried out the first experiments on the Gekko laser system, with the results published in 2011 [10]. These experiments used 100 J of laser energy to generate an ablated plume from a thin CH (plastic) foil [10]. The radiation from this plume ionized and ablated a second CH foil, creating a counter-streaming flow [10]. The interaction of the two flows created structures inferred to arise from the collisionless shock produced via the electrostatic instability [6,10]. Shortly thereafter, a series of high power laser experiments were carried out at the Omega laser facility, both on OMEGA and OMEGA EP, in which the team has observed properties of counter-propagating plasma with low interflow collisionality generated by laser ablation of opposing thin foils using 5 kJ per target laser energies [26]. Proton radiography in these experiments has shown evidence of field structure [28]. Experiments have also been carried out on a single ablated plasma to understand the plasma conditions generated in each independent flow of the counter-streaming case [26,29]. This characterization is critical to experimental analysis of the collisionless system. Papers by H S Park et al. [26], J S Ross et al. [29], and N L Kugland et al. [28] have extensively discussed the results of these experiments.

Work by Ryutov et al. [25], Park, et al. [26], and Drake and Gregori [6] lay out a semi-analytical analysis of experimental requirements to produce Weibel-mediated shocks for collisionless interpenetrating ablated flows. In the present paper, three critical criteria for the generation of a Weibel-mediated collisionless shocks are discussed: obtaining the required density and experimental length scale [6,25,26], maintaining low enough interflow collisionality to remain in the collisionless regime [6,25,26], and obtaining the necessary growth rates of the Weibel instability [6]. The first two criteria will be discussed below in assessing the feasibility of collisionless shock generation. The first criterion refers to the fact that the size of the system must be large enough to accommodate the length scale for Weibel instability growth. The area in which the ablated flows interact determines the size of the system and the growth length scale is set by the ion skin depth for the plasma, with PIC simulations suggesting the need for 300 skin depths within the interaction region in order to obtain a fully-formed Weibel-mediated collisionless shock [19–21]. For a given ablated plasma material, the skin depth varies proportional to $N_e^{-1/2}$, where N_e is the electron density; therefore the plasma density must be large in order to make the skin depth short enough to meet the criterion [6]. The other criterion that we discuss is ensuring that the system maintains low interflow collisionality. The ion mean free path, $\lambda_{\rm mfp}$, for interpenetrating flows is approximately

$$\lambda_{\rm mfp}({\rm cm}) \sim 5\times 10^{-12}\frac{A_Z^2}{Z^4}\frac{[v({\rm cm/s})]^4}{n_Z({\rm cm^{-3}})\ln\Lambda}\cos^4\frac{\alpha}{2} \tag{1}$$

where A_Z is the atomic weight, Z is the atomic number, υ is the relative bulk flow velocity of the plasmas, n_Z is the total ion density, and α is the intersection angle of the two flows. The Coulomb logarithm will be evaluated from

$$\ln\Lambda = \max\left[1, \left(35 - \ln\left[\frac{Z^2(2A_Z)c^2}{A_Z^2 v^2}\sqrt{\frac{Zn_{Z1}}{T_{\rm keV}}}\right]\right)\right] \tag{2}$$

for counter-streaming flows with the same composition and where n_{Z1} refers to a single flow density. The ion mean free path depends on the flow velocity much more strongly than on the plasma density. As such, in order to meet the two necessary criteria to be discussed, we must show that the plasma flow is sufficiently fast and dense for the formation of a collisionless shock by the Weibel instability.

3. Computational modeling with the CRASH code

We have utilized the CRASH code to explore experimental parameters for the single foil, laser-ablated plasmas at the OMEGA [30] laser facility, as well as for the NIF [31]. As we will show, while CRASH is not currently able to model the dynamics which lead to the Weibel instability and collisionless shock formation in these high-energy-density experiments, the radiation-hydrodynamics and laser energy deposition models in CRASH appear to be capable of accurately describing the macroscale plasma evolution relevant to this case. The results from CRASH simulations can be used to evaluate plasma properties of the ablated flow given different target geometries and experimental parameters, as will be discussed below. This is important both for assessing designs of potential experimental campaigns at high-energy-density facilities and for gaining some insight into those parameters that are difficult to diagnose experimentally.

The CRASH code is a semi-implicit radiation-hydrodynamics code with adaptive mesh refinement [32] that has been used to model radiative shocks [33,34], as well as a variety of other high-energy-density physics systems [35,36]. Details of the CRASH physics model can be found in papers by Van der Holst et al. [32,37]. A brief summary of the physics utilized for simulations in this paper follows. We utilized the implicit multigroup radiation transport with 10 photon energy groups. The relatively sparse photon group resolution was used to limit computational time and because energy transport of specific groups does not play an important role in the system of interest here. The simulations utilize a tabular equation-of-state (EOS), either using tables generated by a dedicated EOS model for the CRASH predictive science project or tables from an external model. The only plastic that has been developed for the CRASH project as such is polyimide, therefore for models of the plastic foil targets, the equation-of-state for polyimide is used in place of a table for the specific plastic. The comparison between the CRASH model and the experimental data discussed below will justify this approximation. Runs utilizing equation-of-state tables for the specific plastics in the experiment using the PROPACEOS model developed by Prism Inc. are under development. The CRASH laser package is capable of both 2D *R-Z* and fully 3D laser ray tracing. Additionally, the code is able to do the full 3D ray tracing and map the laser energy deposition back to the 2D geometry mesh. Early simulations of these laser ablation experiments were carried out before the development and testing of the 3D-to-2D capability, thus utilized the *R-Z* beam geometry. The simulations in this paper have been carried out with the *R-Z* geometry beams in order to maintain a consistent laser physics model throughout the runs. Future runs will utilize the 3D-to-2D laser package. In the reported simulation results, the laser spatial profile was a super-Gaussian with a power of 4.2. The reported radius is half of the full width at half maximum of this spatial profile. The rays were incident at 21.7° from normal to the target surface to allow for some effect of laser refraction from non-normal rays through the corona. Because CRASH is an Eulerian hydrodynamics code, the cells must be initialized with some mass; as such, the cells representing the vacuum that surrounds the target experimentally contain low density material, utilizing the same equation-of-state as the target material.

4. Simulation of experiments carried out at the OMEGA facility

In order to assess the ability of the CRASH code to model the laser ablation experiments, we utilized data from December 2009 experiments on the OMEGA 60 laser published by J S Ross et al. [29]. Single foil and double foil experiments were carried out on 0.5 mm thick CH_2 foils, driving the ablated flow with nominally 4.7 kJ of laser energy in a 1 ns pulse with a 250 μm diameter spot. The main diagnostic was Thomson scattering, which measures the electron and ion density, as well as the electron and ion temperature, ionization state, and flow velocity from a finite scattering volume. Further Thomson scattering details can be found in the Ross et al. paper [29], as well as a 1999 paper by Glenzer et al. [38]. In the 2009 experiments, the scattering volume was approximately a 100 μm cube located 4 mm from the foil surface, 4 mm from each foil in the two-foil case, along the central axis of the laser beam spot [29].

In order to model the single foil experiments just described, we utilized a computational domain in the *R-Z*, axially-symmetric geometry, spanning from −4.5 mm to 0.5 mm in the axial direction and from 0.0 mm to 1.0 mm in the radial direction The domain utilized reflecting boundary conditions on the symmetry axis and float boundaries on all others. The laser rays in the calculation travel in the positive *Z*-direction, therefore the ablated flow is traveling in the negative *Z*-direction. The plasma conditions to be compared to experimental data were extracted by averaging over the zones within a 50 μm radius of the central axis, 4 mm from the target surface. The calculations utilized the adaptive mesh refinement in the CRASH code with a 64 μm base resolution, refining on steep density and temperature gradients. Calculations carried out at 3 through 6 maximum AMR levels showed that the plasma variables at the diagnostic region showed little variation above 4 levels corresponding to a 4 μm resolution.

Fig. 1 shows a comparison between CRASH and the experimental data for the experiments at 4712 J. Fig. 1a shows that the electron density predicted by CRASH is in good agreement with the experimental data for the range of the simulation. The maximum electron density in both the simulation and the data peaks at $5 \times 10^{18}\ \mathrm{cm}^{-3}$ around 5 ns and slowly drops to $4 \times 10^{18}\ \mathrm{cm}^{-3}$ by 8–9 ns. Fig. 1b displays the flow velocity versus time for the simulation with the experimental data overlaid. While this is expected because the ablated flow is approximately a homologous flow and thus the velocity falls off at approximately as $1/t$ where t is the time experimental time, it is nevertheless an important test to assure that the model is faithfully representing the system, and that the timing for the two systems is in agreement. Lastly, from Fig. 1c we can see that the ion temperature is in reasonable agreement with the experimental data near 3 ns, but the ions in the simulation do not maintain as high a temperature as the experiment, falling to roughly 15 eV by 9 ns whereas the data indicates a temperature holding between 30 eV and 50 eV. This discrepancy is possibly due to details in the equation-of-state model and will be further investigated. The electron temperature cannot be compared between the systems because it is believed that the Thomson scattering probe laser heats the electrons, providing an artificial minimum temperature and leading to a discrepancy between models and experimental measurements [26]. Overall, the strong agreement between CRASH and experimental data is considered more than adequate for use of this model in design of further experiments investigating collisionless counter-streaming plasmas generated by laser ablation.

5. Simulation of potential experiments on the NIF

Because the NIF allows for a large increase in available energy to drive the experiments, it has been speculated that experiments may reach the regime necessary to form a Weibel-mediated collisionless shock [6,26]. In preparation for planned experiments on the NIF, a series of simulations have been carried out to assess the feasibility of this claim. The two criteria we will be using to judge this possibility are the characteristic length for the instability growth and the mean free path for ions in the interpenetrating flows. As discussed previously, the ion skin depth determines the characteristic length for a collisionless shock formation, with PIC simulations by Spitkovsky as well as Kato and Takabe concluding that a threshold of 300 ion skin depths within the interacting region was necessary [19–21]. Experiments unable to reach this length scale would not provide the space necessary for the Weibel instability to isotropize the particle flow and form a collisionless shock; however, evidence of magnetic field filamentation by the Weibel instability might still be observable. We must also assure that the collisionality in between particles in the interpenetrating flows remains low and as such want the mean free path for ion–ion collisions to remain long compared to the interaction region between the flows [6,25,26].

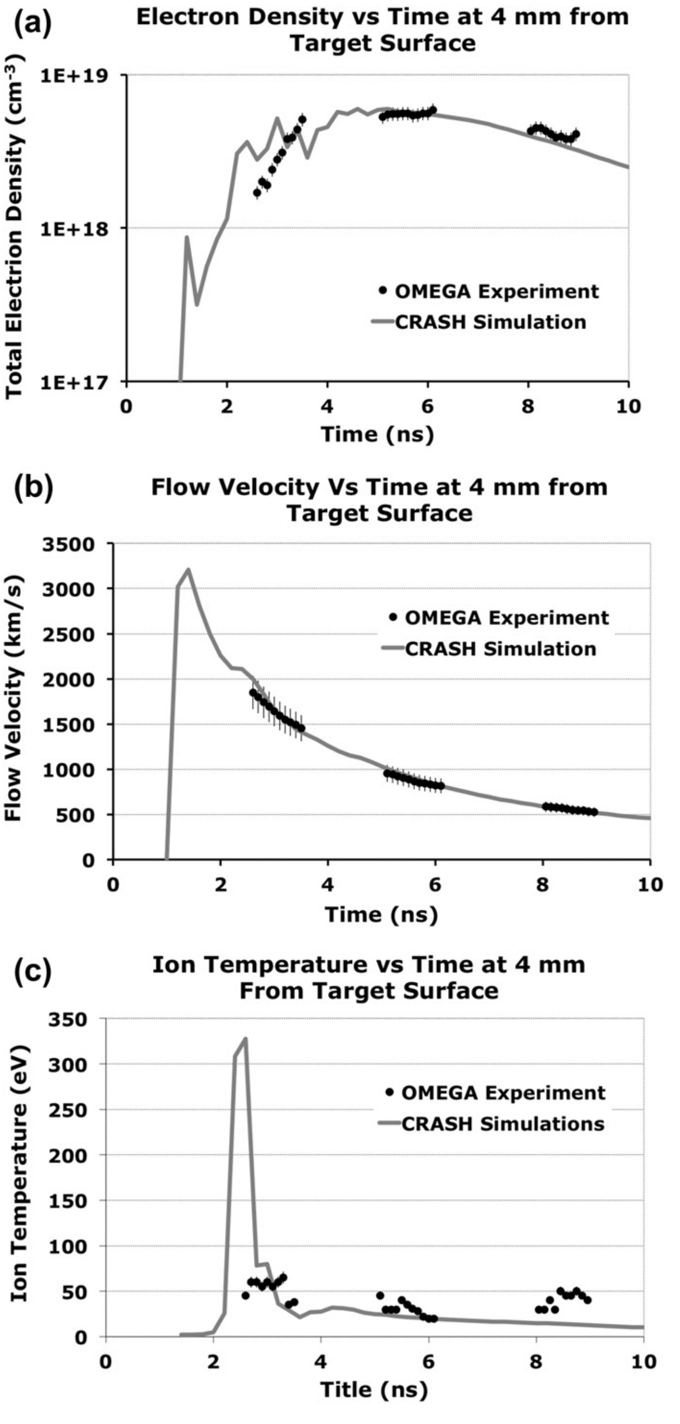

Fig. 1. These plots display the electron density (a), the flow velocity (b), and the ion temperature (c) versus time for the ablated plasma a distance of 4 mm from the foil surface driven by 4712 J with a 1 ns pulse. The results of CRASH simulations show good agreement with experimental data in the three variables, though the ion temperature cools more quickly in the models.

Two simulation results are reported here. In both cases a single, 2 mm thick plastic foil is irradiated by 500 kJ of laser energy in a 600 μm radius spot. The first case presented delivers the energy in a 1 ns drive pulse, whereas the second delivers the same energy but in a 10 ns drive pulse, leading to an order of magnitude lower irradiance. As in the previously discussed simulations of the OMEGA experiments, the computational domain extends out 4.5 mm from the target surface in the ablation direction. Ideally this would extend further for the NIF models, but computational cost limited the domain extent. Future simulations will explore longer domains through better optimization of code parameters. The plasma conditions to be analyzed will be extracted near the symmetry axis in the *R-Z* coordinate system. The data for the 1 ns drive case will be presented out to the full 20 ns experimental window, however the 10 ns drive case is limited to the first 4.4 ns of the model due to time constraints.

We will first discuss the results of the model for the 1 ns drive pulse. Fig. 2 shows how the plasma conditions 4 mm from the target surface vary in time. This location is chosen in part because it is near the end of the domain and in part to compare to the previously presented OMEGA results. The total electron density, shown in Fig. 2a, is shown to climb to 6×10^{20} cm^{-3} near 4 ns before tailing to 1×10^{20} cm^{-3} by 20 ns, roughly two orders of magnitude higher than the electron density reached in the OMEGA experiments. The velocity curve, shown in Fig. 2b, matches that of the OMEGA experiment, maintaining flow velocity above 1000 km/s until 5 ns and falling off as t^{-1}. The model indicates that the ion temperature peaks briefly to nearly 4 keV at 3.2 ns before dropping under 1 keV at 4.4 ns and reaching 100 eV at 11.4 ns.

To assess the criteria for generation of a Weibel-mediated collisionless shock, we calculate the ion skin depth and ion mean free path using the assumptions made in the published design analyses [6,25,26]. The ion mean free path and ion skin depth for a given

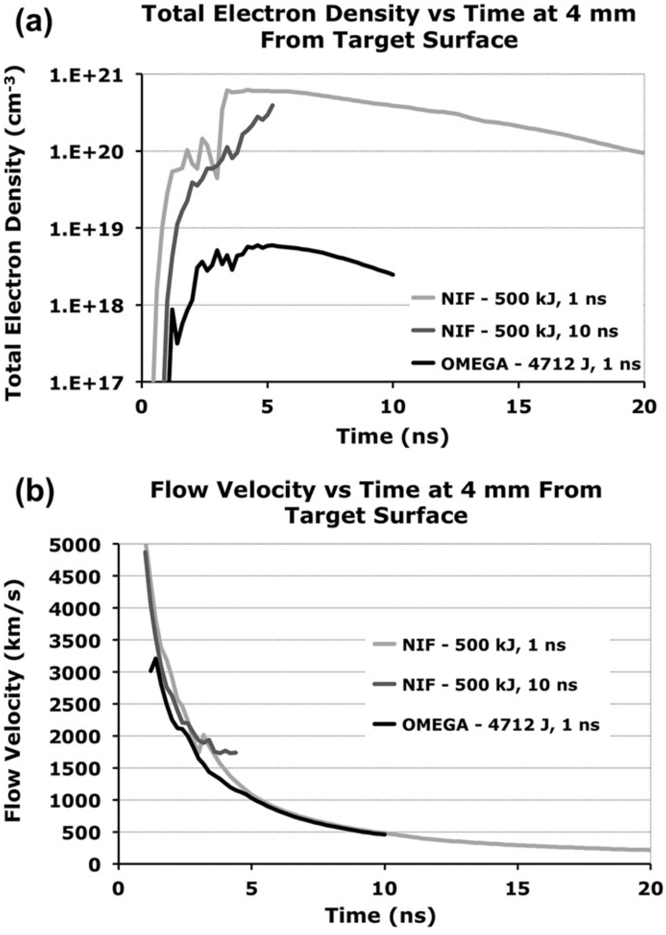

Fig. 2. These plots display the electron density (a) and flow velocity (b) versus time for the ablated plasma a distance of 4 mm from the foil surface driven with three different laser parameters. The CRASH models of the NIF experimental conditions reach two orders of magnitude higher electron densities than the OMEGA model, while maintaining velocities above 1000 km/s for 5 ns.

target separation will be calculated by the plasma state in the simulation at half the separation distance. This allows us to assess the range of possible target separations and range of times that would feasibly allow the formation of the collisionless shock. This analysis will use the interaction region as defined in Drake and Gregori, where interaction region is defined as half the target separation distance centered at the midpoint between the foils [6]. Fig. 3 shows a color-contour plot of the number of ion skin depths within the interaction region with the axes varying target separation horizontally and time vertically. Fig. 3 clearly displays the regions where the target separation indicates that greater than the requisite 300 ion skin depths fit within the interaction region, as specified by criteria 1, as well as the regions where the ion mean free path is much longer than the interaction region, thus meeting criteria 2. For target separations greater than 3 mm, there exists a region where both criteria are met for the 1 ns drive. For an 8 mm target separation, a window from 3 ns until 10 ns exists in which both criteria 1 and criteria 2 are met, indicating that the generation of a collisionless shock is feasible for this experimental configuration, assuming that there is actually enough Weibel instability growth, which seems likely from Drake and Gregori [6]. The chart also indicates that it may be possible to meet the criteria for longer durations with larger target separation, though this cannot be confirmed due to the computational domain. At later times, a region of target separation that meets criteria 1 also exists; however, because the fluid velocity is small in this region, the collisionality remains too high to generate collisionless shocks.

In the second simulation, the laser drive used the same energy and spot size, but was sustained for 10 ns. This led to a lower irradiance, but a sustained source of ablation until later times. Unfortunately, the model results have not been carried out for the full 20 ns because of computational constraints. Fig. 2 shows the early time results of this simulation run as compared with the 1 ns data. It is important to note that the simulation is approaching and appears will reach the same peak electron density (Fig. 2a), but because of the longer, sustained drive, the simulation indicates the possibility of higher velocity (Fig. 2b) for a prolonged time. Because the collisionality drops proportional to v^4, this suggests that the longer drive would allow the simulation to stay in the Weibel-mediated collisionless shock regime for more time.

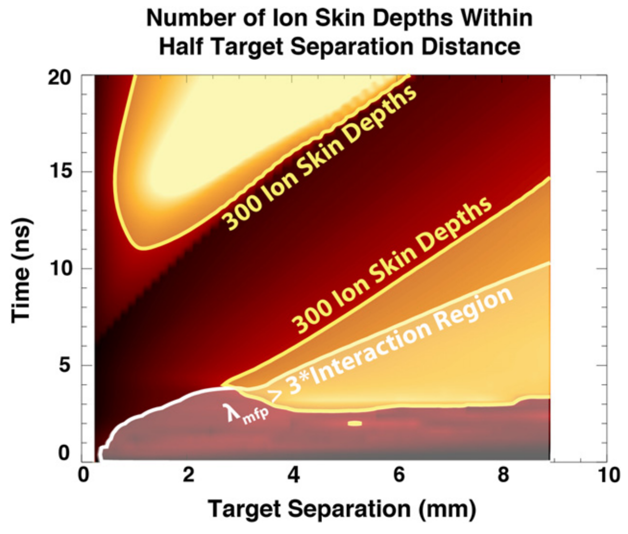

Fig. 3. The number of ion skin depths, which controls the scale length for growth of the collisionless shock, is plotted versus target separation and time. The 300 ion skin depth contours (shaded) indicate the areas in which the scale length for the collisionless shock formation is less than the interaction region of the two plasmas. A second shaded contour is shown which indicates the locations where the mean free path for ions, λ_{mfp}, is greater than 3 times the size of the interaction region. The area in which these contours overlap shows the regions where both the collisionality and experimental scale length criteria are met for this CRASH model.

6. Summary and conclusion

Simulations using the CRASH code indicate that ablation experiments using laser parameters possible on the NIF are capable of meeting critical criteria necessary for the development of a collisionless shock mediated by the Weibel instability in a well-controlled laboratory experiment. These simulations are supported by a close comparison between simulated and experimental data from experiments on Omega. For a pulse duration of 1 ns, the model suggests that a target separation of 8 mm would allow for a 7 ns window during which a collisionless shock could form before the system is no longer in the low interflow collisionality regime. Furthermore, the simulations indicate that delivering the same total energy in a longer drive may allow for an extended timeframe in which the collisionless shock would be able to exist.

CRASH simulations to obtain a more detailed coverage of the laser parameter space are underway with the goal of optimizing the likelihood and duration of collisionless shock formation in the upcoming experimental campaign. Additionally, models of the interpenetrating flows and models utilizing the MHD capabilities of the CRASH code are being considered and tested.

Acknowledgments

This work is funded by the Predictive Sciences Academic Alliances Program in NNSA-ASC via grant DEFC52-08NA28616 and by the NNSA-DS and SC-OFES Joint Program in High-Energy-Density Laboratory Plasmas, grant number DE-FG52-09NA29548. Partial support from the European Research Council grant agreement no. 256973 is acknowledged.

References

[1] R.A. Treumann, Fundamentals of collisionless shocks for astrophysical application, 1. non-relativistic shocks, Astronomy and Astrophysics Review 17 (2009) 409–535. Times cited: 17 R.A. Treumann.
[2] A.M. Bykov, R.A. Treumann, Fundamentals of collisionless shocks for astrophysical application, 2. relativistic shocks, Astronomy and Astrophysics Review 19 (2011). Times cited: 9 A.M. Bykov, R.A. Treumann.
[3] R. Petre, Evidence for cosmic ray acceleration in supernova remnants from X-ray observations, in: S. Holt, U. Hwang (Eds.), Young Supernova Remnants, vol. 565, American Inst. Phys., 2000, pp. 360–368.
[4] R.Z. Sagdeev, Cooperative phenomena and shock waves in collisionless plasmas, Reviews of Plasma Physics 4 (1966) 23.
[5] R.P. Drake, The design of laboratory experiments to produce collisionless shocks of cosmic relevance, Physics of Plasmas 7 (2000) 4690–4698.
[6] R.P. Drake, G. Gregori, Design considerations for unmagnetized collisionless-shock measurements in homologous flows, The Astrophysical Journal 749 (2012) 171.
[7] F. Fiuza, R.A. Fonseca, J. Tonge, W.B. Mori, L.O. Silva, Weibel-instability-mediated collisionless shocks in the laboratory with ultraintense lasers, Physical Review Letters 108 (2012) 235004.
[8] A. Bell, P. Choi, A. Dangor, O. Willi, D. Bassett, C. Hooker, Collisionless shock in a laser-produced ablating plasma, Physical Reviews A 38 (1988) 1363–1369.
[9] T. Morita, Y. Sakawa, Y. Kuramitsu, S. Dono, H. Aoki, H. Tanji, T.N. Kato, Y.T. Li, Y. Zhang, X. Liu, J.Y. Zhong, H. Takabe, J. Zhang, Collisionless shock generation in high-speed counterstreaming plasma flows by a high-power laser, Physics of Plasmas 17 (2010) 122702.
[10] Y. Kuramitsu, Y. Sakawa, T. Morita, C.D. Gregory, J.N. Waugh, S. Dono, H. Aoki, H. Tanji, M. Koenig, N. Woolsey, H. Takabe, Time evolution of collisionless shock in counterstreaming laser-produced plasmas, Physical Review Letters 106 (2011) 175002.
[11] X. Liu, Y.T. Li, Y. Zhang, J.Y. Zhong, W.D. Zheng, Q.L. Dong, M. Chen, G. Zhao, Y. Sakawa, T. Morita, Y. Kuramitsu, T.N. Kato, L.M. Chen, X. Lu, J.L. Ma, W.M. Wang, Z.M. Sheng, H. Takabe, Y.J. Rhee, Y.K. Ding, S.E. Jiang, S.Y. Liu, J.Q. Zhu, J. Zhang, Collisionless shockwaves formed by counter-streaming laser-produced plasmas, New Journal of Physics 13 (2011) 093001.
[12] D.B. Schaeffer, E.T. Everson, D. Winske, C.G. Constantin, A.S. Bondarenko, L.A. Morton, K.A. Flippo, D.S. Montgomery, S.A. Gaillard, C. Niemann,

Generation of magnetized collisionless shocks by a novel, laser-driven magnetic piston, Physics of Plasmas 19 (2012). Times cited: 0 D.B. Schaeffer, E.T. Everson, D. Winske, C.G. Constantin, A.S. Bondarenko, L.A. Morton, K.A. Flippo, D.S. Montgomery, S.A. Gaillard, C. Niemann.

[13] D. Haberberger, S. Tochitsky, F. Fiuza, C. Gong, R.A. Fonseca, L.O. Silva, W.B. Mori, C. Joshi, Collisionless shocks in laser-produced plasma generate monoenergetic high-energy proton beams, Nature Physics 8 (2012) 95–99. Times cited: 4 Haberberger, Dan Tochitsky, Sergei Fiuza, Frederico Gong, Chao Fonseca, Ricardo A. Silva, Luis O. Mori, Warren B. Joshi, Chan.

[14] D.W. Forslund, C.R. Shonk, Formation and structure of electrostatic collisionless shocks, Physical Review Letters 25 (1970) 1699–1702.

[15] L.O. Silva, M. Marti, J.R. Davies, R.A. Fonseca, C. Ren, F.S. Tsung, W.B. Mori, Proton shock acceleration in laser-plasma interactions, Physical Review Letters 92 (2004) 015002.

[16] T.N. Kato, H. Takabe, Electrostatic and electromagnetic instabilities associated with electrostatic shocks: two-dimensional particle-in-cell simulation, Physics of Plasmas 17 (2010) 032114.

[17] E.S. Weibel, Spontaneously growing transverse waves in a plasma due to an anisotropic velocity distribution, Physical Review Letters 2 (1959) 83–84.

[18] M.V. Medvedev, A. Loeb, Generation of magnetic fields in the relativistic shock of gamma-ray burst sources, The Astrophysical Journal 526 (1999) 697.

[19] T.N. Kato, H. Takabe, Nonrelativistic collisionless shocks in unmagnetized electron-ion plasmas, The Astrophysical Journal Letters 681 (2008) L93.

[20] H. Takabe, T.N. Kato, Y. Sakawa, Y. Kuramitsu, T. Morita, T. Kadono, K. Shigemori, K. Otani, H. Nagatomo, T. Norimatsu, S. Dono, T. Endo, K. Miyanishi, T. Kimura, A. Shiroshita, N. Ozaki, R. Kodama, S. Fujioka, H. Nishimura, D. Salzman, B. Loupias, C. Gregory, M. Koenig, J.N. Waugh, N.C. Woolsey, D. Kato, Y.-T. Li, Q.-L. Dong, S.-J. Wang, Y. Zhang, J. Zhao, F.-L. Wang, H.-G. Wei, J.-R. Shi, G. Zhao, J.-Y. Zhang, T.-S. Wen, W.-H. Zhang, X. Hu, S.-Y. Liu, Y.K. Ding, L. Zhang, Y.-J. Tang, B.-H. Zhang, Z.-J. Zheng, Z.-M. Sheng, J. Zhang, High-mach number collisionless shock and photo-ionized non-lte plasma for laboratory astrophysics with intense lasers, Plasma Physics and Controlled Fusion 50 (2008) 124057.

[21] A. Spitkovsky, On the structure of relativistic collisionless shocks in electron-ion plasmas, The Astrophysical Journal Letters 673 (2008) L39.

[22] P. Chang, A. Spitkovsky, J. Arons, Long-term evolution of magnetic turbulence in relativistic collisionless shocks: electron-positron plasmas, The Astrophysical Journal 674 (2008) 378.

[23] A. Spitkovsky, Particle acceleration in relativistic collisionless shocks: fermi process at last? The Astrophysical Journal Letters 682 (2008) L5.

[24] L. Gargate, R.A. Fonseca, J. Niemiec, M. Pohl, R. Bingham, L.O. Silva, The nonlinear saturation of the non-resonant kinetically driven streaming instability, The Astrophysical Journal Letters 711 (2010) L127.

[25] D.D. Ryutov, N.L. Kugland, H.-S. Park, S.M. Pollaine, B.A. Remington, J.S. Ross, Collisional current drive in two interpenetrating plasma jets, Physics of Plasmas 18 (2011) 104504.

[26] H.-S. Park, D. Ryutov, J. Ross, N. Kugland, S. Glenzer, C. Plechaty, S. Pollaine, B. Remington, A. Spitkovsky, L. Gargate, G. Gregori, A. Bell, C. Murphy, Y. Sakawa, Y. Kuramitsu, T. Morita, H. Takabe, D. Froula, G. Fiksel, F. Miniati, M. Koenig, A. Ravasio, A. Pelka, E. Liang, N. Woolsey, C. Kuranz, R. Drake, M. Grosskopf, Studying astrophysical collisionless shocks with counter-streaming plasmas from high power lasers, High Energy Density Physics 8 (2012) 38–45.

[27] N.L. Kugland, D.D. Ryutov, C. Plechaty, J.S. Ross, H.-S. Park, Invited article: relation between electric and magnetic field structures and their proton-beam images, Review of Scientific Instruments 83 (2012a) 101301–101301-26.

[28] N.L. Kugland, D.D. Ryutov, P.-Y. Chang, R.P. Drake, G. Fiksel, D.H. Froula, S.H. Glenzer, G. Gregori, M. Grosskopf, M. Koenig, Y. Kuramitsu, C. Kuranz, M.C. Levy, E. Liang, J. Meinecke, F. Miniati, T. Morita, A. Pelka, C. Plechaty, R. Presura, A. Ravasio, B.A. Remington, B. Reville, J.S. Ross, Y. Sakawa, A. Spitkovsky, H. Takabe, H.-S. Park, Self-organized electromagnetic field structures in laser-produced counter-streaming plasmas, Nature Physics (2012) (advance online publication).

[29] J.S. Ross, S.H. Glenzer, P. Amendt, R. Berger, L. Divol, N.L. Kugland, O.L. Landen, C. Plechaty, B. Remington, D. Ryutov, W. Rozmus, D.H. Froula, G. Fiksel, C. Sorce, Y. Kuramitsu, T. Morita, Y. Sakawa, H. Takabe, R.P. Drake, M. Grosskopf, C. Kuranz, G. Gregori, J. Meinecke, C.D. Murphy, M. Koenig, A. Pelka, A. Ravasio, T. Vinci, E. Liang, R. Presura, A. Spitkovsky, F. Miniati, H.-S. Park, Characterizing counter-streaming interpenetrating plasmas relevant to astrophysical collisionless shocks, Physics of Plasmas 19 (2012) 056501.

[30] T. Boehly, D. Brown, R. Craxton, R. Keck, J. Knauer, J. Kelly, T. Kessler, S. Kumpan, S. Loucks, S. Letzring, F. Marshall, R. McCrory, S. Morse, W. Seka, J. Soures, C. Verdon, Initial performance results of the omega laser system, Optics Communications 133 (1997) 495–506.

[31] E.I. Moses, Ignition on the national ignition facility, Journal of Physics: Conference Series 112 (2008) 012003.

[32] B. van der Holst, G. Tth, I.V. Sokolov, K.G. Powell, J.P. Holloway, E.S. Myra, Q. Stout, M.L. Adams, J.E. Morel, S. Karni, B. Fryxell, R.P. Drake, Crash: a block-adaptive-mesh code for radiative shock hydrodynamics implementation and verification, The Astrophysical Journal Supplement Series 194 (2011) 23.

[33] R. Drake, F. Doss, R. McClarren, M. Adams, N. Amato, D. Bingham, C. Chou, C. DiStefano, K. Fidkowski, B. Fryxell, T. Gombosi, M. Grosskopf, J. Holloway, B. van der Holst, C. Huntington, S. Karni, C. Krauland, C. Kuranz, E. Larsen, B. van Leer, B. Mallick, D. Marion, W. Martin, J. Morel, E. Myra, V. Nair, K. Powell, L. Rauchwerger, P. Roe, E. Rutter, I. Sokolov, Q. Stout, B. Torralva, G. Toth, K. Thornton, A. Visco, Radiative effects in radiative shocks in shock tubes, High Energy Density Physics 7 (2011) 130–140.

[34] J.P. Holloway, D. Bingham, C.-C. Chou, F. Doss, R.P. Drake, B. Fryxell, M. Grosskopf, B. van der Holst, B.K. Mallick, R. McClarren, A. Mukherjee, V. Nair, K.G. Powell, D. Ryu, I. Sokolov, G. Toth, Z. Zhang, Predictive modeling of a radiative shock system, Reliability Engineering and System Safety 96 (2011) 1184–1193 (Quantification of Margins and Uncertainties).

[35] E.M. Rutter, M.J. Grosskopf, G. Malamud, C.C. Kuranz, E.C. Harding, P.A. Keiter, R.P. Drake, Comparison between Kelvin-Helmholtz instability experiments on OMEGA and simulation results using the CRASH code, High Energy Density Physics 9 (2013) 148–151.

[36] M.R. Trantham, C.C. Kuranz, G. Malamud, M.J. Grosskopf, E.S. Myra, R.P. Drake, A.R. Miles, H.-S. Park, B.A. Remington, Simulations of radiative effects on the Rayleigh-Taylor instability using the CRASH code, High Energy Density Physics 9 (2) (2013) 303–308.

[37] B. van der Holst, G. Toth, I.V. Sokolov, B.R. Torralva, K.G. Powell, R.P. Drake, M. Klapisch, M. Busquet, B. Fryxell, E.S. Myra, Simulating radiative shocks with the CRASH laser package, High Energy Density Physics 9 (2013) 8–16.

[38] S.H. Glenzer, W.E. Alley, K.G. Estabrook, J.S.D. Groot, M.G. Haines, J.H. Hammer, J.-P. Jadaud, B.J. MacGowan, J.D. Moody, W. Rozmus, L.J. Suter, T.L. Weiland, E.A. Williams, Thomson scattering from laser plasmas, Physics of Plasmas 6 (1999) 2117–2128.